PHILOSOPHICAL TRANSACTIONS OF THE ROYAL SOCIETY A
MATHEMATICAL, PHYSICAL & ENGINEERING SCIENCES

# Ly*a* absorption systems and the intergalactic medium

G. Efstathiou, J. Schaye and T. Theuns

*Phil. Trans. R. Soc. Lond. A* 2000 **358**, 2049-2062
doi: 10.1098/rsta.2000.0629

10.1098/rsta.2000.0629





# Ly$\alpha$ absorption systems and the intergalactic medium

By G. Efstathiou[1], J. Schaye[1] and T. Theuns[1,2]

[1]*Institute of Astronomy, Madingley Road, Cambridge CB3 0HA, UK*

[2]*Max-Plank-Institut für Astrophysik, Postfach 1523, 85740 Garching, Germany*

The last few years have seen a dramatic improvement in our understanding of the origin of Ly$\alpha$ absorption systems. Hydrodynamic numerical simulations of cold-dark-matter-dominated universes have shown that the many properties of the Ly$\alpha$ absorption systems can be explained by a photoionized, space-filling, intergalactic medium. Ly$\alpha$ lines offer promising probes of the photoionizing background, the amplitude of the mass fluctuations at high redshift and the evolution of the equation of state of the intergalactic medium.

**Keywords: intergalactic medium; galaxy formation; dark matter**

## 1. Introduction

The existence of a forest of absorption lines blueward of the Ly$\alpha$ emission line in quasar spectra has been known for over 30 years (Bahcall & Salpeter 1965; Lynds 1971). These lines arise from Ly$\alpha$ absorption by neutral hydrogen from intervening structure along the line of sight. Early theoretical models interpreted this structure as absorption caused by discrete gas clouds in the intergalactic medium (IGM), either pressure confined by a hot IGM (Sargent *et al*. 1980; Ostriker & Ikeuchi 1983) or confined by the gravity of dark matter 'mini-halos' (see, for example, Rees 1986). Over the last few years our understanding of the Ly$\alpha$ forest has undergone a transformation for at least two reasons. Firstly, observations with the Keck telescope have produced almost noise-free spectra of quasars at high spectral resolution over the redshift range $2 \lesssim z \lesssim 4$. The exquisite quality of Keck spectra has allowed observers to resolve Ly$\alpha$ absorption lines at low column densities (*ca*. $10^{12.5}$ cm$^{-2}$) and to study their evolution. Secondly, hydrodynamic numerical simulations of structure formation in cold-dark-matter (CDM) universes with high spatial resolution are now possible and have proved remarkably successful in reproducing many observed properties of the Ly$\alpha$ forest (Cen *et al*. 1994; Zhang *et al*. 1995, 1997; Miralda-Escudé *et al*. 1996; Hernquist *et al*. 1996; Theuns *et al*. 1998*a*). These simulations have shown that most of the Ly$\alpha$ lines at column densities $\lesssim 10^{14.5}$ cm$^{-2}$ arise from modest fluctuations in the baryon density in a space-filling photoionized IGM, rather than from distinct clouds. The properties of the Ly$\alpha$ lines can, therefore, be used to probe the structure and thermal history of the diffuse IGM and of the background ultraviolet (UV) radiation that determines its ionization state. The key characteristics of the numerical simulations are described in the next section. Section 3 summarizes a number of

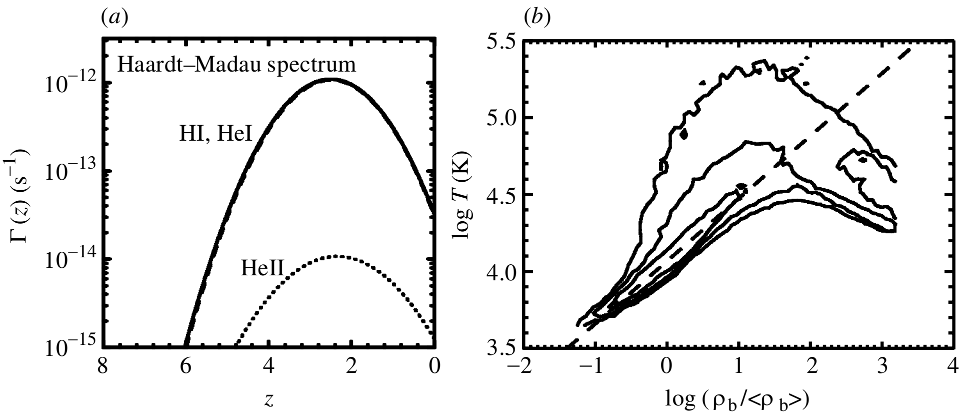


Figure 1. (*a*) Photoionization rates for hydrogen and helium computed in the model of Haardt & Madau (1996). (*b*) The mass-weighted distribution of fluid elements in the temperature–density plane at $z = 3$ for our reference CDM model. The number density of fluid elements increases by an order of magnitude with each contour level. Most of the gas obeys a well-defined equation of state, shown by the dashed line.

results from these simulations and describes how the Ly$\alpha$ lines can be used to study the IGM. In this paper we discuss only the properties of the low-column-density Ly$\alpha$ lines. For a discussion of damped Ly$\alpha$ systems and metal lines see Pettini (this issue). For a recent review of observations and theoretical models of Ly$\alpha$ absorption lines see Rauch (1998).

## 2. Numerical simulations of the IGM

The simplest cosmological hydrodynamical simulations follow the evolution of (optically thin) gas and dark matter assuming a uniform photoionizing background. The simulation is, therefore, specified by

(i) parameters defining the cosmological model and its matter content (e.g. $\Omega_m$, $\Omega_b$, $\Omega_\Lambda$, $H_0 \equiv 100h$ km s$^{-1}$ Mpc$^{-1}$);

(ii) the amplitude and spectral shape of the mass fluctuations; and

(iii) a model for the background UV flux as a function of redshift.

Here we will review the evolution of CDM universes with initially scale-invariant adiabatic fluctuations. The linear power spectrum for these models (in the limit of small baryon content) is given by Bardeen *et al.* (1986). We adopt a reference model (model S) with parameters $\Omega_m = 1$, $\Omega_\Lambda = 0$, $h = 0.5$ and $\Omega_b = 0.05$. The physical density in baryons in this model is $\omega_b \equiv \Omega_b h^2 = 0.0125$. The model is normalized so that the root mean square density fluctuations in spheres of radius $8h^{-1}$ Mpc is $\sigma_8 = 0.7$. The photoionizing background radiation is assumed to originate from quasars according to the model of Haardt & Madau (1996, hereafter HM). The photoionization rates for hydrogen and helium in this model are plotted in figure 1*a* as a function of redshift. With these photoionization rates, and assuming a uniform IGM, hydrogen is reionized at a redshift of $z \approx 6$ and HeII is reionized at $z \approx 4.5$.

Figure 1*b* shows the distribution of gas elements in the temperature–density plane in a numerical simulation of our reference model S at a redshift of $z = 3$. There is a plume of shock-heated gas extending to temperatures $\gtrsim 10^5$ K, but most of the gas has a low overdensity and follows a power-law-like 'equation of state' (Hui & Gnedin 1997):

$$T = T_0(\rho_{\rm b}/\bar{\rho}_{\rm b})^{\gamma-1}. \tag{2.1}$$

At times long after reionization, the diffuse IGM will settle into a state in which adiabatic cooling is balanced by photoheating. The temperature of the IGM will, therefore, tend towards

$$\left.\begin{aligned} T &\approx 3.2\times10^4\ \mathrm{K}\left[\frac{\Omega_{\rm b}h(1+\delta)(1+z)^3}{(2+\alpha)E(z)}\right]^{1/1.76}, \\ E(z) &= \frac{H_0}{H(z)} = [\Omega_{\rm m}(1+z)^3+\Omega_k(1+z)^2+\Omega_\Lambda]^{1/2}, \end{aligned}\right\} \tag{2.2}$$

where we have assumed a power-law photoionizing background

$$J_\nu = J_{\nu_{\rm L}}(\nu/\nu_{\rm L})^{-\alpha}. \tag{2.3}$$

In equation (2.2) $\Omega_k = 1 - \Omega_{\rm m} - \Omega_\Lambda$, and the exponent 1/1.76 arises from the temperature dependence of the HII and HeIII recombination coefficients.

Figure 2 shows the spatial distribution of the gas in the simulation at $z = 3$. Figure 2*b* shows the gas with temperature $T > 10^5$ K. This hot gas fills a small fraction of the volume and is located in the dense knots and filaments corresponding to collapsed structures. In contrast, the cool gas with $T < 10^5$ K (shown in figure 2*b*) fills most of the computational volume. It is this diffuse low-density gas that we believe accounts for the vast majority of the observed Ly$\alpha$ lines. Furthermore, because most of this gas is at low overdensities, $\delta \lesssim 10$, it is relatively easy to model numerically. By investigating the Ly$\alpha$ forest we can, therefore, hope to learn about the properties of the diffuse IGM, which at typical quasar redshifts of $z \sim 2$–4 contains most of the baryonic matter in the Universe. In particular:

(i) the optical depth of HI and HeII absorption can set constraints on the baryonic density of the Universe and on the evolution, amplitude and spectrum of the photoionizing background;

(ii) the fluctuating optical depth of HI absorption can be used to construct the power spectrum of the matter fluctuations at redshifts $z \sim 2$–4; and

(iii) the Ly$\alpha$ absorption linewidths can be used to infer the temperature and equation of state of the diffuse IGM and its evolution.

These topics will be discussed in more detail in the next section.

## 3. The Ly$\alpha$ forest as a probe of the IGM

### (*a*) *Mean optical depth of* HI *and* HeII *absorption*

The optical depth for HI Ly$\alpha$ absorption from an IGM in ionization equilibrium with density $\rho_{\rm b}$ is given by

$$\tau(z) = 6.5\times10^{-4}\left(\frac{\omega_{\rm b}}{0.019}\right)^2\left(\frac{h}{0.65}\right)^{-1}\frac{(1+z)^6}{E(z)}\frac{T_4^{-0.76}}{(\Gamma_{\rm HI}/10^{-12}\ \mathrm{s}^{-1})}\left(\frac{\rho_{\rm b}(z)}{\bar{\rho}_{\rm b}(z)}\right)^2, \tag{3.1}$$

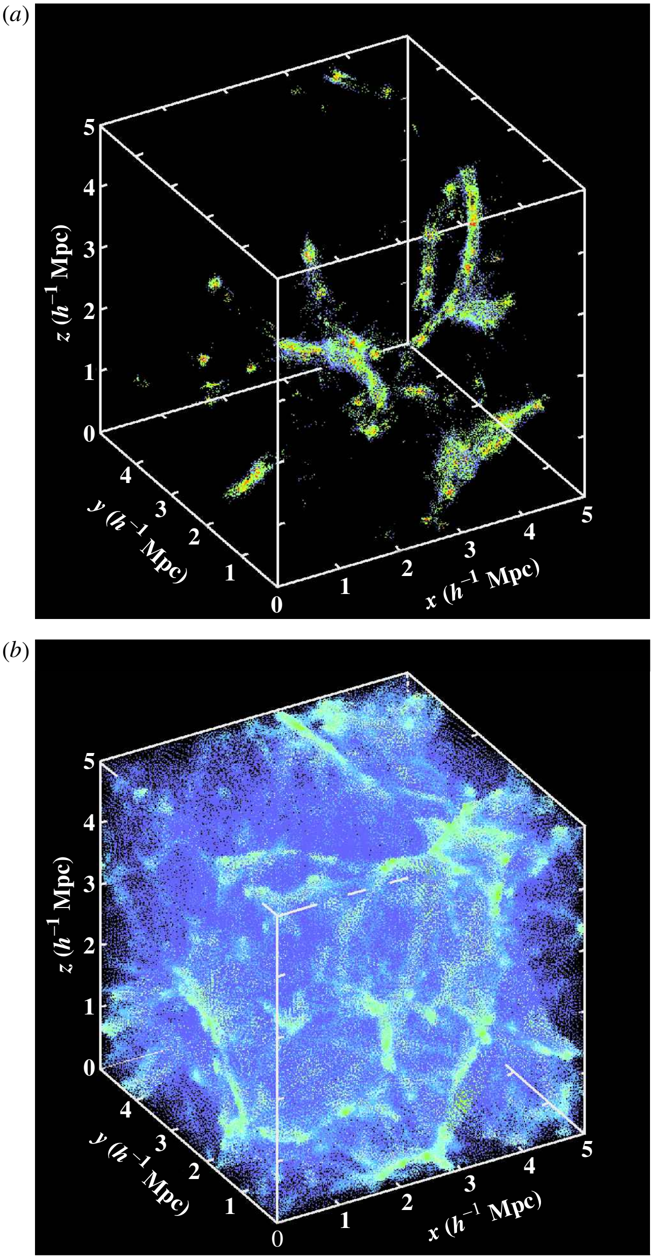


Figure 2. The distribution of gas in a CDM simulation at $z = 3$. (*a*) Shocked gas with a temperature greater than $10^5$ K, which is located in dense clusters and filaments. (*b*) Gas with a temperature of less than $10^5$ K.

(see, for example, Peebles 1993, § 23), where $\Gamma_{\rm HI}$ is the photoionization rate for HI and $T_4$ is the temperature of the IGM in units of $10^4$ K. Variations in $\rho_{\rm b}(z)$ along the line of sight will produce a 'fluctuating Gunn–Peterson' effect. An observed




PHILOSOPHICAL TRANSACTIONS OF THE ROYAL SOCIETY A MATHEMATICAL, PHYSICAL & ENGINEERING SCIENCES

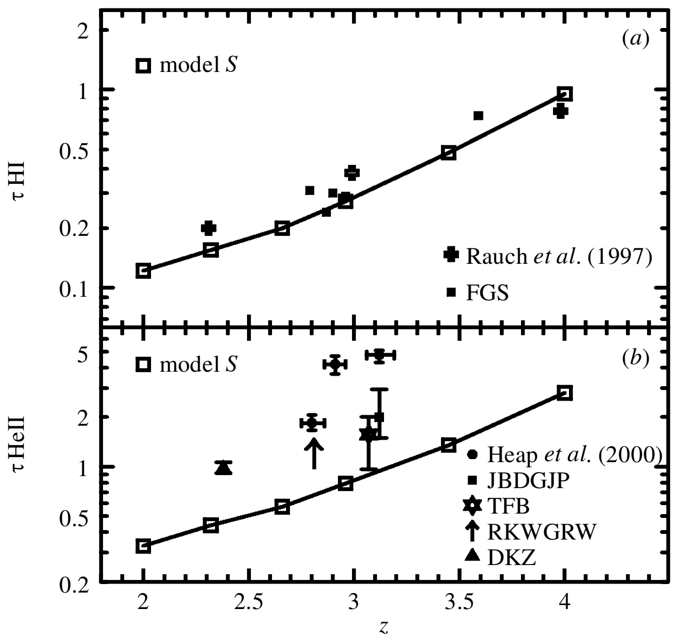


Figure 3. The mean optical depth as a function of redshift for HI and HeII absorption. Our reference model S (using half the amplitude of the HM photoionizing background) is plotted as the open squares joined by the solid line. This matches the observed HI optical depth but fails to match observations of the HeII optical depth. The observational data plotted in the figure are as follows: Rauch *et al.* (1997); Fardal *et al.* (1998) (FGS); Davidsen *et al.* (1996) (DKZ); Jakobsen *et al.* (1994) (JBDGJP); Reimers *et al.* (1997) (RKWGRW); Tytler *et al.* (1995) (TFB); Heap *et al.* (2000).



absorption line spectrum can, therefore, be inverted to infer the clustering of the baryon distribution as pioneered by Croft *et al.* (1998; see also § 3 *c* below).

The mean HI and HeII optical depths as a function of redshift are plotted in figure 3 for our fiducial model S. The open squares show the optical depths derived using half the amplitude of the HM UV background. With this choice of photoionizing background, the mean HI optical depth of the simulation matches observations quite well over the redshift range 2–4. Evidently, the amplitude of the photoionizing background can be balanced by variations in other cosmological parameters according to equation (3.1) to preserve the match to observations. The simulations therefore imply that

$$\left(\frac{\omega_{\rm b}}{0.0125}\right)^2 \left(\frac{h}{0.5}\right)^{-1} \Omega_{\rm m}^{1/2} \left(\frac{0.5\Gamma_{\rm HM}}{\Gamma_{\rm HI}}\right) \left(\frac{6\times10^3}{T}\right)^{0.76} \approx 1. \tag{3.2}$$

This type of criterion has been used by Weinberg *et al.* (1997) to set a crude lower limit to the baryon density. At redshifts of 2–3 one can be reasonably confident of the HM model of the photoionizing background around the Lyman edge, because the quasar luminosity function is quite well determined at these redshifts (see § 3 of Madau, this issue). The HM model provides a lower limit to the photoionizing flux because it ignores additional photoionizing radiation from star formation. The temperature of a photoionized IGM cannot exceed a few times $10^4$ K, but its precise value depends on the past thermal and ionization history of the IGM.† Uncertainties in the temperature of the IGM lead to an additional source of uncertainty in using equation (3.2) to derive a bound on the baryon density. Nevertheless, equation (3.2) implies $\omega_b \gtrsim 0.02\Omega_m^{1/2}$, interestingly close to the baryon density of $\omega_b = 0.019$ inferred from primordial nucleosynthesis and the deuterium abundances measured in quasar spectra (Burles & Tytler 1998; Burles *et al*. 1999). The observed HI optical depth, therefore, leads to a consistent picture in which most of the baryons in the Universe at $z \sim 2$–4 belong to the diffuse photoionized IGM.

The HeII optical depth is shown in figure 3*b*. The open squares show $\tau_{\rm HeII}$ computed from the simulation using the same amplitude for the photoionizing background that provides a good match to $\tau_{\rm HI}$. The results from the simulation lie below the observations at all redshifts, suggesting that the photoionizing background has a softer spectrum than that computed by Haardt & Madau (1996). In photoionization equilibrium, the optical depth in HeII is related to the optical depth in HI by $\tau_{\rm HeII}/\tau_{\rm HI} \propto \Gamma_{\rm HI}/\Gamma_{\rm HeII} \propto J_{\rm HI}/J_{\rm HeII}$, and so $\tau_{\rm HeII}$ can be raised by softening the photoionizing spectrum appropriately. By lowering $\Gamma_{\rm HeII}/\Gamma_{\rm HI}$ by a factor of two compared with the HM model of figure 1, model S can match the observations at $z \lesssim 2.8$, but cannot match the high HeII optical depths at $z \gtrsim 2.9$ found in the recent observations by the Hubble Space Telescope (HST) and the Space Telescope Imaging Spectrograph (STIS) of the quasar Q0302-003 by Heap *et al*. (2000).

One possible interpretation of these results is that the typical quasar spectrum adopted by Haardt & Madau (1996) is too hard and that HeII reionization is delayed until a redshift of $z \approx 3$, corresponding to the abrupt change in HeII opacity observed by Heap *et al*. (2000). Additional arguments to support this picture are discussed in § 3 *d*. If this interpretation is correct, then active galactic nuclei (AGN) and 'mini-quasars' cannot produce much photoionizing radiation capable of doubly ionizing helium at redshifts of $z \gtrsim 3$ (see Rees, this issue).

### (*b*) *Evolution of the column density distribution*

It has been known for many years that a Ly$\alpha$ forest shows strong cosmological evolution (see, for example, Sargent *et al*. 1980). Over a narrow range in redshift the evolution can be approximated by a power law,

$$\frac{dN}{dz} \propto (1+z)^{\epsilon}, \tag{3.3}$$

where $N$ is the number of lines above a threshold rest-frame equivalent width (typically $W > 0.32$ Å). From high-resolution Keck observations, Kim *et al*. (1997) found $\epsilon = 2.78 \pm 0.71$ in the redshift range $2 < z < 3.5$. Williger *et al*. (1994) found that the evolution is still stronger at higher redshifts with $\epsilon > 4$ at $z > 4$. In contrast, observations with the HST indicate much weaker evolution at low redshifts with $\epsilon = 0.48 \pm 0.62$ for $z < 1$ (Morris *et al*. 1991; Bahcall *et al*. 1991, 1993; Impey *et al*. 1996).

The evolution of the Ly$\alpha$ forest, including the low rates of evolution at redshifts of $z \lesssim 2$ can be reproduced quite simply in CDM models (Theuns *et al*. 1998*b*; Davé *et al*. 1999). This is illustrated in figure 4, which shows the evolution of the number

† Although a highly ionized IGM is in ionization equilibrium, it is not in thermal equilibrium and so retains a 'memory' of the way in which it was heated.

of Ly$\alpha$ lines within a given range of column density for our reference model S. (The lines are identified by fitting Voigt profiles to simulated Keck spectra using the line-fitting program VPFIT (Webb 1987).) As in § 3 *a*, we adopt the HM model of the photoionizing background with an amplitude divided by a factor of 2 to match the observed optical depth in HI absorption. This model reproduces the observed column density distribution accurately over the column density range $10^{12.5}\ \mathrm{cm}^{-2} \lesssim N_{\mathrm{HI}} \lesssim 10^{15}\ \mathrm{cm}^{-2}$ (see fig. 2 in Theuns *et al.* (1998*b*)), and, as figure 4 shows, also reproduces the observed rates of evolution as a function of column density. In particular, the decrease in the rate of evolution of the Ly$\alpha$ lines found from HST observations arises from the steep decline in the photoionizing background at $z \lesssim 2$ caused by the rapid drop in quasar numbers at low redshift.

### (*c*) *Reconstruction of the matter power spectrum*

Equations (2.1) and (3.1) can be combined to write the observed transmitted flux in terms of fluctuations in the baryon density:

$$F = \exp[-A(\rho_{\mathrm{b}}/\bar{\rho}_{\mathrm{b}})^{\beta}], \qquad \beta \approx (2.76 - 0.76\gamma). \tag{3.4}$$

Croft *et al.* (1998) have used this relation to infer the one-dimensional power spectrum $P_{\mathrm{1D}}(k)$ of the baryon fluctuations, from which the three-dimensional power spectrum can be recovered by differentiation:

$$P(k) = -\frac{2\pi}{k}\frac{\mathrm{d}}{\mathrm{d}k}P_{\mathrm{1D}}(k). \tag{3.5}$$

Croft *et al.* (1998) calibrate the amplitude of the matter power spectrum by comparing it with numerical simulations. The procedure is not completely straightforward and we refer the reader to Croft *et al.* (1998) for details. By testing their inversion algorithm against numerical simulations these authors find that the amplitude and shape of the underlying matter power spectrum can be recovered accurately and that the recovery is insensitive to uncertainties in the equation of state. A variant of this technique, which incorporates a correction for the distortion of the clustering pattern by peculiar velocities, is described by Nusser & Haehnelt (1999).

Croft *et al.* (1999*b*) describe an application of their method to a sample of 19 quasar spectra spanning the redshift range 2.08–3.23. They recover $P(k)$ at $z \approx 2.5$ over the (comoving) wavenumber range $2\pi/k \sim 2$–$12h^{-1}$ Mpc and find that it is well fitted by a power law $P(k) \propto k^n$ with $n = -2.25 \pm 0.28$, consistent with what is expected from CDM models. This important result is the first attempted determination of the matter power spectrum at high redshift. The amplitude of the inferred power spectrum is high compared with that expected for spatially flat CDM models with $\Omega_{\mathrm{m}} = 1$ normalized to reproduce the abundance of rich clusters at the present day. The best-fitting CDM models have $\Omega_{\mathrm{m}} + 0.2\Omega_{\Lambda} \approx 0.46$ (Weinberg *et al.* 1999; Phillips *et al.* 2000), in agreement with the parameters $\Omega_{\mathrm{m}} \approx 0.3$, $\Omega_{\Lambda} \approx 0.7$ derived from combining observations of anisotropies in the cosmic microwave background radiation and distant Type Ia supernovae (see, for example, Efstathiou *et al.* (1999), and references therein). Constraints on neutrino masses from estimates of $P(k)$ at high redshift are discussed by Croft *et al.* (1999*a*).

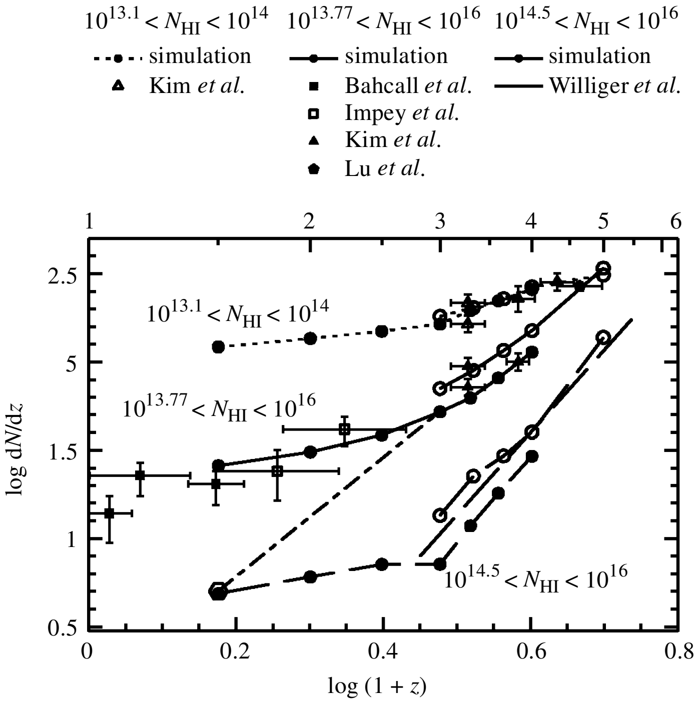


Figure 4. Evolution of the number of lines within a given range of column density from numerical simulations of Theuns *et al.* (1998*b*) compared with observations. Open and filled circles show simulation results for the reference model S (described in the text) run at different numerical resolutions. The large open pentagon shows a re-analysis of the simulation at $z = 0.5$ but imposing the photoionizing background appropriate to $z = 2$. The observational data points are as follows: Kim *et al.* (1997) (open and filled triangles); Bahcall *et al.* (1993) (filled squares); Impey *et al.* (1996) (open squares); Lu *et al.* (1996) (filled pentagon); Williger *et al.* (1994) (long-dashed line).

### (*d*) *Widths of the Ly$\alpha$ lines*

The widths of the Ly$\alpha$ lines are usually characterized by the broadening parameter $b$ determined by fitting Voigt profiles. If the linewidth is caused by thermal broadening, the parameter $b$ is related to the temperature of the gas by

$$b = \left(\frac{2kT}{m_p}\right)^{1/2} = 12.8T_4^{1/2}\ \mathrm{km\ s^{-1}}. \tag{3.6}$$

In reality, a number of mechanisms in addition to thermal broadening contribute to the widths of the lines, e.g. the differential Hubble flow across the absorbing region and the smoothing of small-scale fluctuations by gas pressure (Bryan *et al.* 1999; Theuns *et al.* 2000).

The first sets of simulations of the Ly$\alpha$ forest in CDM models appeared to show good agreement with the observed $b$-parameter distributions. However, subsequent simulations with higher spatial resolution produced a larger fraction of narrower lines than observed (Theuns *et al.* 1998*a*; Bryan *et al.* 1999). This is illustrated in figure 5, which shows observations of the $b$ distribution at $z \approx 3$ compared with the results

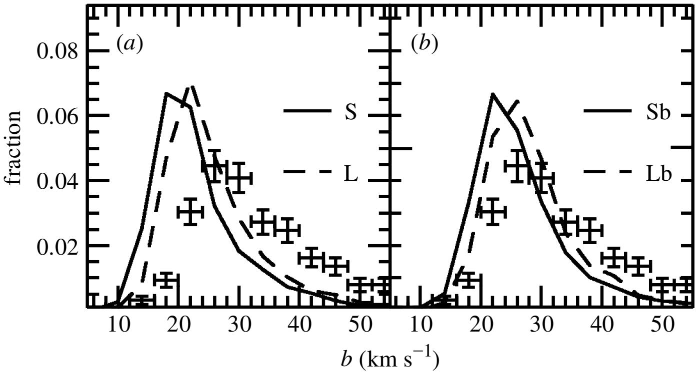


Figure 5. ($a$) The distribution of linewidths at $z = 3$ derived from simulations of the reference model S and for a spatially flat $\Lambda$-dominated universe (model L) with $\Omega_\Lambda = 0.7$ and identical photoionizing background. Both of these models have a baryon density of $\omega_{\mathrm{b}} = 0.0125$. ($b$) Models with $\omega_{\mathrm{b}} = 0.025$ and with double the amplitude of the photoionizing background so that the optical depth of HI absorption is almost unchanged. The error bars show observational results from Hu *et al*. (1995).

from numerical simulations. Figure 5$a$ shows the distribution derived by fitting Voigt profiles to simulated spectra from reference model S (solid line). The lines in this model are clearly too narrow, suggesting that the temperature of the IGM is too low. From the asymptotic relation (2.2) one can see that the temperature of the IGM can be raised by increasing the baryon density and by lowering $\Omega_{\mathrm{m}}$ (the asymptotic temperature is extremely insensitive to the amplitude of the photoionizing background long after reionization). Figure 5$b$ shows the effect of increasing the baryon density to $\omega_{\mathrm{b}} = 0.025$. The dashed lines in both parts of figure 5 show the effect of lowering $\Omega_{\mathrm{m}}$ and introducing a cosmological constant so that the Universe remains spatially flat. These variations in cosmological parameters can go some way to resolving the conflict with observations (Theuns *et al*. 1999), but cannot provide an exact match unless the baryon density is much higher than the value favoured from primordial nucleosynthesis. This suggests that we are missing a significant heating source of the IGM. A number of mechanisms have been suggested that might boost the temperature of the IGM, e.g. photoelectric heating of dust grains (Nath *et al*. 1999) and Compton heating by the hard X-ray background (Madau & Efstathiou 1999). However, the most plausible explanation (Abel & Haehnelt 1999) is that the simulations underestimate the temperature at $z \sim 3$ because they assume an optically thin IGM (and also a uniform photoionizing background that has *already* been reprocessed by Ly$\alpha$ absorbing clouds; see Haardt & Madau (1996)). This is inconsistent and the simulations should properly include the effects of radiative transfer while the medium is still optically thick prior to complete reionization, because in this regime every photoionizing photon is absorbed and contributes to heating the IGM. Abel & Haehnelt (1999) estimate that correct inclusion of radiative transfer during the epoch of HeII reionization might increase the temperature of the IGM by a factor of approximately 2, perhaps enough to resolve the discrepancy with the observed $b$-parameter distributions illustrated in figure 5. The idea that the temperature of the IGM at $z \sim 3$ is boosted by HeII reionization is supported by the analysis of the equation of state of the IGM described in the next subsection.





PHILOSOPHICAL TRANSACTIONS OF THE ROYAL SOCIETY A MATHEMATICAL, PHYSICAL & ENGINEERING SCIENCES

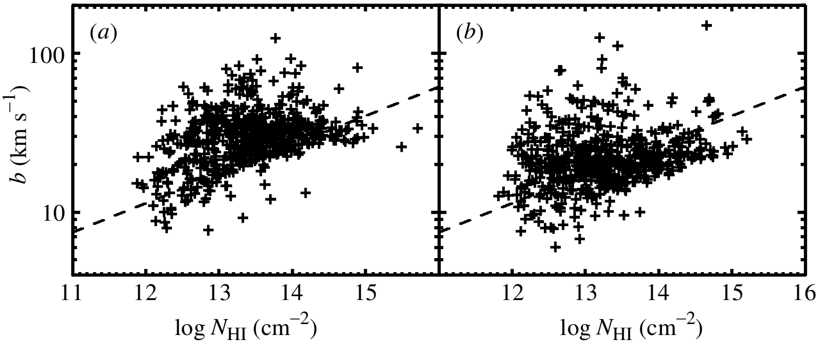


Figure 6. The $b(N)$ distributions derived by applying the Voigt profile-fitting program VPFIT to 800 random lines of sight through two cosmological simulations at $z = 3$. (*a*) The results for a model with a hot IGM (see text). Only lines with VPFIT errors $\Delta b/b < 0.5$ and $\Delta N_{\rm HI}/N_{\rm HI} < 0.5$ are plotted. The dashed line shows the best fit to the lower envelope of the $b(N)$ distribution over the column density range $10^{12.5}$ cm$^{-2}$ $\leqslant N_{\rm HI} \leqslant 10^{14.5}$ cm$^{-2}$ determined using the algorithm of Schaye *et al.* (1999). This dashed line is reproduced in part (*b*) together with the $b(N)$ distribution for the colder reference model S.

## (*e*) *Constraining the equation of state of the IGM*

As we have mentioned, a number of physical mechanisms contribute to the breadth of the $b$ distribution. However, the minimum linewidth is set by the temperature of the gas, which in turn depends on the density (cf. figure 1). By fitting the cut-off in the $b$ distribution as a function of column density (the '$b(N)$' distribution), one can reconstruct the effective equation of state of the IGM (Schaye *et al.* 1999; Ricotti *et al.* 2000; Bryan & Machacek 2000).

The method is illustrated in figure 6, which shows the $b(N)$ distributions derived by applying the VPFIT line-fitting program to two cosmological simulations. Results for the standard reference model S are plotted in figure 6*b*. Figure 6*a* shows a hotter model, which has the same parameters as model Lb plotted in figure 5 but with the HeI and HeII photoheating rates doubled over those of the HM model (crudely representing 'radiative transfer' effects during the reionization of helium). The dashed line in the figure shows the best fit to the lower envelope of the $b(N)$ distribution of figure 6*a*, determined by applying the iterative fitting algorithm of Schaye *et al.* (1999). The same line is plotted in figure 6*b* and it passes almost through the middle of the $b(N)$ distribution of the colder model. The lower envelope of the $b(N)$ distribution is clearly a sensitive indicator of the characteristic temperature of the Ly$\alpha$ clouds and can be accurately determined from fits to high-resolution quasar spectra.

What is more difficult is to convert the fit to the lower envelope of the $b(N)$ distribution, $b = b_0(N/N_0)^{\Gamma-1}$, into the parameters $T_0$ and $\gamma$ of the effective equation of state of the IGM (equation (2.1)). This is done by calibrating $b_0$ and $\Gamma$ against $T_0$ and $\gamma$ using numerical simulations with different equations of state (see Schaye *et al.* (1999) for details).

The results of applying this technique to nine high-quality quasar spectra spanning the redshift range $2.0 < z < 4.5$ are shown in figure 7 (Schaye *et al.* 2000). Except for the two lowest redshift quasars, the Ly$\alpha$ forest spectra were divided in two to reduce the effects of redshift evolution and signal-to-noise variations across a single spectrum. From $z \sim 3.5$ to $z \sim 3$, the inferred temperature at the mean density of

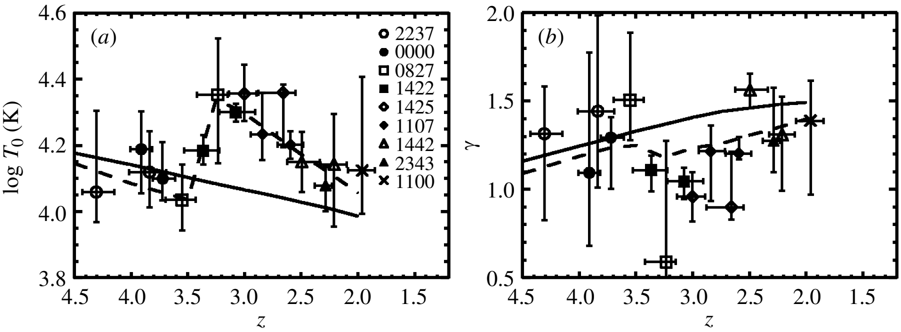


Figure 7. ($a$) The temperature at the mean density as a function of (decreasing) redshift inferred from the lower envelope in the $b(N)$ distribution determined from nine high-resolution spectra (Schaye *et al.* 2000). ($b$) The inferred slope of the equation of state as a function of redshift. The horizontal error bars indicate the redshift interval spanned by the absorption lines, and the vertical error bars show estimates of 1$\sigma$ errors. The lines show the evolution of the equation of state in two numerical simulations as described in the text. Different symbols correspond to different quasars.

the IGM, $T_0$, increases and the gas is close to isothermal ($\gamma \sim 1$). This behaviour differs markedly from that expected if helium were fully reionized at higher redshift. For example, the solid lines show the evolution of the equation of state in a simulation with the HM background. In this simulation, both hydrogen and helium are fully ionized by $z \approx 4.5$ and the temperature of the IGM declines slowly as the Universe expands, tending to the asymptotic form of equation (2.2). This model cannot account for the peak in the temperature at $z \sim 3$ inferred from the observations. Instead, we associate the peak in $T_0$, and the low value of $\gamma$, with reheating caused by the second reionization of helium (HeII → HeIII). This interpretation is supported by the abrupt change in HeII opacity at $z \sim 3$ from the measurements of Heap *et al.* (2000) discussed in § 3 *a*. It is also consistent with evidence from the SiIV/CIV ratio that the spectrum of the photoionizing background hardens abruptly at $z \sim 3$ (Songaila & Cowie 1996; Songaila 1998).†

The dashed lines in figure 7 show a 'designer model' with parameters tuned to fit the observations. This simulation has a much softer UV background at high redshift than the model shown by the solid line, and, consequently, HeII reionizes at $z \sim 3.2$. In addition, the photoheating rates have been enhanced during reionization to boost the temperature of the IGM (again, crudely modelling the heating of optically thick gas). This model suggests that the jump in temperature at $z \sim 3$ may be associated with HeII reionization, but, clearly, more-realistic simulations that include radiative transfer are required to determine the evolution of the equation of state during the reionization phase more accurately. Further observations would also be useful to assess how steeply the IGM temperature changes between $z = 4$ and $z = 3$.

## 4. Summary and outlook

The work reviewed in this paper provides a powerful argument that the Lyα forest arises from a space-filling, highly photoionized, diffuse IGM that contains most of the

† Note, however, that Boksenberg *et al.* (1998) found a more gradual change of the SiIV/CIV ratio with redshift.

baryonic material in the Universe at high redshift. This model is a natural outcome of CDM theories of structure formation and can account for many observed properties of the Ly$\alpha$ forest in quantitative detail. The general features of the model thus seem to us to be reasonably secure.

However, a more detailed analysis of the thermal history of the IGM requires simulations that incorporate radiative transfer, and a model for the spatial distribution of ionizing sources. Such calculations are now being done (Abel *et al.* 1999; Gnedin 2000; Madau, this issue), but the computational problems are formidable. Some outstanding problems that deserve further attention are listed below.

(i) Detailed simulations of the inhomogeneous reionization of H and He.

(ii) Extending the analysis of Ly$\alpha$ linewidths to redshifts $\gtrsim 4$, perhaps leading to constraints on the epoch of reionization of hydrogen.

(iii) Analysis of inhomogeneities in the temperature of the IGM. Are there, for example, regions in the spectra of quasars in which Ly$\alpha$ linewidths are systematically broader or narrower than in other regions?

(iv) Further observations of absorption gaps in HeII Ly$\alpha$ absorption (reported by Heap *et al.* (2000) and others) and the development of a model to understand their sizes.

(v) Searching for signatures of outflows around protogalaxies in the Ly$\alpha$ forest.

(vi) Determining the mean metallicity of the IGM and understanding how the metals were transported from protogalaxies.

J.S. thanks the Isaac Newton Trust for financial support and the PPARC for the award of a studentship. We also thank Anthony Leonard, Michael Rauch and Wal Sargent for their contributions to this work.

## References

Abel, T. & Haehnelt, M. G. 1999 *Astrophys. J.* **520**, L13.
Abel, T., Norman, M. L. & Madau, P. 1999 *Astrophys. J.* **523**, 66.
Bahcall, J. N. & Salpeter, E. E. 1965 *Astrophys. J.* **142**, 1677.
Bahcall, J. N., Jannuzi, B. T., Schneider, D. P., Hartig, G. F., Bohlin, R. & Junkkarinen, V. 1991 *Astrophys. J.* **377**, L5.
Bahcall, J. N. *et al.* 1993 *Astrophys. J. Suppl.* **87**, 1.
Bardeen, J. M., Bond, J. R., Kaiser, N. & Szalay, A. S. 1986 *Astrophys. J.* **304**, 15.
Boksenberg, A., Sargent, W. L. W. & Rauch, M. 1998 Preprint (astro-ph/9810502). In *Proc. Xth Rencontres de Blois.* (In the press.)
Bryan, G. L. & Machacek, M. E. 2000 *Astrophys. J.* **534**, 57.
Bryan, G. L., Machacek, M. E., Anninos, P. & Norman, M. L. 1999 *Astrophys. J.* **517**, 13.
Burles, S. & Tytler, D. 1998 *Astrophys. J.* **499**, 699.
Burles, S., Kirkman, D. & Tytler, D. 1999 *Astrophys. J.* **519**, 18.
Cen, R., Miralda-Escudé, J., Ostriker, J. P. & Rauch, M. 1994 *Astrophys. J.* **437**, L83.
Croft, R. A. C., Weinberg, D. H., Katz, N. & Hernquist, L. 1998 *Astrophys. J.* **495**, 44.
Croft, R. A. C., Hu, W. & Davé, R. 1999*a* *Phys. Rev. Lett.* **83**, 1092.

Croft, R. A. C., Weinberg, D. H., Pettini, M., Hernquist, L. & Katz, N. 1999*b* *Astrophys. J.* **520**, 1.

Davé, R., Hernquist, L., Katz, N. & Weinberg, D. H. 1999 *Astrophys. J.* **511**, 521.

Davidsen, A. F., Kriss, G. A. & Zheng, W. 1996 *Nature* **380**, 47.

Efstathiou, G., Bridle, S. L., Lasenby, A. N., Hobson, M. P. & Ellis, R. S. 1999 *Mon. Not. R. Astr. Soc.* **303**, L47.

Fardal, M. A., Giroux, M. L. & Shull, J. M. 1998 *Astr. J.* **115**, 2206.

Gnedin, N. Y. 2000 *Astrophys. J.* (In the press.)

Haardt, F. & Madau, P. 1996 *Astrophys. J.* **461**, 20.

Heap, S. R., Williger, G. M., Smette, A., Hubeny, I., Sahu, M., Jenkins, E. B., Tripp, T. M. & Winkler, N. 2000 *Astrophys. J.* **534**, 69.

Hernquist, L., Katz, N., Weinberg, D. H. & Miralda-Escudé, J. 1996 *Astrophys. J.* **457**, L51.

Hu, E. M., Kim, T., Cowie, L. L., Songaila, A. & Rauch, M. 1995 *Astr. J.* **110**, 1526.

Hui, L. & Gnedin, N. Y. 1997 *Mon. Not. R. Astr. Soc.* **292**, 27.

Impey, C. D., Petry, C. E., Malkan, M. A. & Webb, W. 1996 *Astrophys. J.* **463**, 473.

Jakobsen, P. *et al.* 1994 *Nature* **370**, 35.

Kim, T., Hu, E. M., Cowie, L. L. & Songaila, A. 1997 *Astron. J.* **114**, 1.

Lu, L., Sargent, W. L. W., Womble, D. S. & Takada-Hidai, M. 1996 *Astrophys. J.* **472**, 509.

Lynds, C. R. 1971 *Astrophys. J.* **164**, L73.

Madau, P. & Efstathiou, G. 1999 *Astrophys. J.* **517**, L9.

Miralda-Escudé, J., Cen, R., Ostriker, J. P. & Rauch, M. 1996 *Astrophys. J.* **471**, 582.

Morris, S. L., Weymann, R. J., Savage, B. D. & Gilliland, R. L. 1991 *Astrophys. J.* **377**, L21.

Nath, B. B., Sethi, S. K. & Shchekinov, Y. 1999 *Mon. Not. R. Astr. Soc.* **303**, 1.

Nusser, A. & Haehnelt, M. 1999 *Mon. Not. R. Astr. Soc.* **303**, 179.

Ostriker, J. P. & Ikeuchi, S. 1983 *Astrophys. J.* **268**, L63.

Peebles, P. J. E. 1993 *Principles of physical cosmology.* Princeton, NJ: Princeton University Press.

Phillips, J., Weinberg, D. H., Croft, R. A. C., Hernquist, L., Katz, N. & Pettini, M. 2000 *Astrophys. J.* (In the press.)

Rauch, M. 1998 *A. Rev. Astron. Astrophys.* **36**, 267.

Rauch, M. *et al.* 1997 *Astrophys. J.* **489**, 7.

Rees, M. J. 1986 *Mon. Not. R. Astr. Soc.* **218**, 25.

Reimers, D., Kohler, S., Wisotzki, L., Groote, D., Rodriguez-Pascual, P. & Wamsteker, W. 1997 *Astron. Astrophys.* **327**, 890.

Ricotti, M., Gnedin, N. Y. & Shull, J. M. 2000 *Astrophys. J.* **534**, 41.

Sargent, W. L. W., Young, P. J., Boksenberg, A. & Tytler, D. 1980 *Astrophys. J. Suppl.* **42**, 41.

Schaye, J., Theuns, T., Leonard, A. & Efstathiou, G. 1999 *Mon. Not. R. Astr. Soc.* **310**, 57.

Schaye, J., Theuns, T., Rauch, M., Efstathiou, G. & Sargent, W. L. W. 2000 *Mon. Not. R. Astr. Soc.* (In the press.)

Songaila, A. 1998 *Astr. J.* **115**, 2184.

Songaila, A. & Cowie, L. L. 1996 *Astr. J.* **121**, 335.

Theuns, T., Leonard, A., Efstathiou, G., Pearce, F. R. & Thomas, P. A. 1998*a* *Mon. Not. R. Astr. Soc.* **301**, 478.

Theuns, T., Leonard, A. & Efstathiou, G. 1998*b* *Mon. Not. R. Astr. Soc.* **297**, L49.

Theuns, T., Leonard, A., Schaye, J. & Efstathiou, G. 1999 *Mon. Not. R. Astr. Soc.* **303**, L58.

Theuns, T., Schaye, J. & Haehnelt, M. G. 2000 *Mon. Not. R. Astr. Soc.* (In the press.)

Tytler, D., Fan, X.-M. & Burles, S. 1995 *Nature* **381**, 207.

Webb, J. K. 1987 QSO absorption lines. PhD thesis, University of Cambridge.

Weinberg, D. H., Miralda-Escudé, J., Hernquis, L. & Katz, N. 1997 *Astrophys. J.* **490**, 564.

Weinberg, D. H., Croft, R. A. C., Hernquist, L., Katz, N. & Pettini, M. 1999 *Astrophys. J.* **522**, 563.

Williger, G. M., Baldwin, J. A., Carswell, R. F., Cooke, A. J. & Hazard, C. 1994 *Astrophys. J.* **428**, 574.

Zhang, Y., Anninos, P. & Norman, M. L. 1995 *Astrophys. J.* **453**, L47.

Zhang, Y., Anninos, P. & Norman, M. L. 1997 *Astrophys. J.* **485**, 496.



PHILOSOPHICAL TRANSACTIONS OF THE ROYAL SOCIETY A MATHEMATICAL, PHYSICAL & ENGINEERING SCIENCES